X-602-76-106
PREPRINT

VLF-EMISSIONS FROM RING CURRENT ELECTRONS

KAICHI MAEDA
PAUL H. SMITH
ROGER R. ANDERSON

MAY 1976

GODDARD SPACE FLIGHT CENTER
GREENBELT, MARYLAND

VLF-EMISSIONS FROM RING-CURRENT ELECTRONS

I. An Interpretation of the "Band of Missing Emissions"

VLF-emissions associated with the enhancement of ring current electrons during magnetic storms and substorms have been detected by the equatorially orbiting S^3-A satellite (Explorer 45).[1,2]

The emissions observed near the geomagnetic equator consist of essentially two frequency regimes, i.e., one above the electron gyrofrequency, f_H, at the equator and the other below f_H. This is indicated in Figure 1 which is a part of the wide-band data obtained during the main phase of the December 17, 1971 magnetic storm.[1] The upper figure is the AC-magnetic field data measured by the search-coil magnetometer with the upper cutoff of 3 kHz[3] and the lower figure is the AC-electric field data obtained by the electric field sensor with the upper cutoff of 10 kHz.[4] These figures show the time sequence of the observed emissions along the inbound orbit (No. 101) of the satellite as f_H changes approximately from 3 kHz at 20 UT to 6 kHz at 21 UT.

The emissions above f_H are electrostatic mode,[5,6,7] which peak near the frequencies of $(n + 1/2)\, f_H$, where n is positive integer, and sometimes emissions up to n = 10 are observed.[2] On the other hand, the emissions below f_H are whistler mode, which have a conspicuous gap along exactly half electron gyrofrequency, $f_H/2$. Although the automatic gain control (AGC) of the sensor makes occasional spurious intensity variations among the emissions, it should be

noticed that the emissions above $f_H/2$ are generally stronger and more continuous than those below $f_H/2$.

The purpose of this short note is first to describe the characteristics of these VLF-emissions and the associated electron intensity enhancements as well as the anisotropies of the ring current electrons, and second to give an interpretation of the bimodal frequency distribution of the equatorial whistler mode emissions. This bimodal distribution has been known for the past few years but not well explained.[8,9]

Another example of the equatorial magnetospheric VLF-emissions is shown in Figure 2. In this figure, the emission data which were observed during the substorm on January 22, 1972 are digitized in one minute averages and are normalized by f_H computed from the onboard magnetometer data. Shown in the upper portion of this figure is the magnetic latitude of the satellite at the time when the emissions shown below are observed. The figures of dark and grey shades correspond to the emissions of electronstatic mode and of whistler mode, respectively. As can be seen from the frequency of occurrence distribution shown on the right side, the whistler mode emission has a bimodal frequency distribution with a sharp dip exactly at the half electron gyrofrequency, $f_H/2$.

The variations of the directional differential electron intensities (cm^{-2} sec^{-1} $ster^{-1}$ keV^{-1}), corresponding to this emission event are shown in Figure 3 for electrons of 90° pitch angle and for electrons with the smallest observable pitch angle

(close to 25°). The difference between these two plots for each energy is a manifestation of the pitch angle anisotropies and is indicated by the vertical hatched lines. The time intervals indicated by horizontal hatched lines and grey shade are the periods when the emissions shown in Figure 2 are observed and when the satellite is inside of the plasmasphere, respectively. A short period inside of the plasmasphere around 7 UT (approximately 20 MLT) represents the double structure of the evening side plasmapause.[2]

From this figure, we can see that the VLF-emissions are observed only when the satellite is outside of the plasmasphere and that the beginning of the emission coincides with the satellite's encounter with the enhanced electron fluxes. It should be noticed, however, that the enhancement of electron intensities associated with the observed VLF-emission is limited to the low energy electrons only (i.e., below 6 keV in this event).

To see the energy spectrum of electrons during this emission event, the flux spectrum at 7:30 UT on January 22, 1972 is plotted in Figure 4. The mean quiet period spectrum observed by this satellite, which has been given by Lyons and Williams (1975)[10] is also plotted for comparison. Approximating these energy spectra and the pitch angle distribution of electrons by

$$j(E,\alpha) \sim E^{-n} \sin^m \alpha \qquad (1)$$

the parameters n and m for three energy regimes are also shown in Figure 4. From this figure. we can see not only the enhancement of the intensity but also the anisotropy is larger in the lower energy electrons.

It should be mentioned here that the growth rate of waves excited by resonant electrons increases with increasing anisotropy of the electrons, and that the peak of emission shift to higher frequency as the anisotropy of the resonant electrons increases, particularly for the soft spectrum electrons. For the electrons given by the equation (1), the peak of emission is above $f_H/2$ for $m \gtrsim 2$ with $n \gtrsim 1$.[11] The emissions above $f_H/2$ can also be excited by the cyclotron instability of the plasma composed of thermal and quasithermal (20 ~ 50 eV) particles if the anisotropy of the quasithermal plasma is suitably large.[12] The S^3-A satellite did not carry, however, onboard detectors that were able to measure these low energy plasma particles.

Since the resonance energy, E_R, for electrons encountering the whistler waves of frequency, f, is given by

$$E_R = E_B \frac{f_H}{f} \left(1 - \frac{f}{f_H}\right)^3 \qquad (2)$$

where

$$E_B = \frac{B^2}{8\pi N} \text{ or } E_B = 250 \left(\frac{f_H}{f_p}\right)^2 \quad \text{(in keV)} \qquad (3)$$

B, N and f_p are the magnetic field intensity, the plasma density (cm^{-3}) and the plasma frequency (in kHz), respectively, the energies of electrons resonating with the whistler waves of frequency $f > f_H/2$ is always smaller than those for $f < f_1/2$. In this sense, the enhanced electrons shown in Figures 3 and 4 are able to excite only the emissions of higher frequencies, i.e., $f \gtrsim f_H/2$ emissions.

On the other hand, due to the roughly 11° tilt of the earth's magnetic dipole axis from the rotation axis and the small inclination (of the order of 4°) of the S^3-A satellite orbit, the emission events are occasionally observed off the equator. Figure 5 shows one example which was observed during the substorm on January 18, 1972. All notations are the same as those used in Figure 2, and as indicated by the line in the upper left, the magnetic latitude of the satellite during the event is larger than 10°.

From this figure, we can see that the frequency distribution above $f_H/2$ differs significantly from those of the near equatorial events, indicating that the off-equator propagation of these emissions above $f_H/2$ in the magnetosphere is non-ducted. On the other hand, the emissions below $f_H/2$ are similar to those observed near the equator. It seems therefore that these waves are in the duct propagation with the upper cut-off of the half local electron gyrofrequency, which has been known by the investigation of whistler propagation by both ground and satellite observations.[13,14,15]

Based on the information described above, the formation of the bimodal frequency distribution of the equatorial whistler mode emissions with a sharp dip at $f_H/2$ can be explained as follows. (i) The emission above $f_H/2$ is produced near the equator by the enhanced ring current electrons, resonating with weak broad-band whistler mode noises existing generally in the region of $3 \lesssim L \lesssim 10$ in the earth's magnetosphere. (ii) The emissions below $f_H/2$ are produced in

similar manner near the equator but slightly outside of the observing location, where the magnetic field is weaker, the corresponding gyrofrequency, f_H', is significantly smaller than that of the observing location, f_H. (iii) Those locally produced emissions with $f > f_H'/2$ propagate unducted off the equator in the magnetosphere, and are reflected back toward the equator from the regions where the lower hybrid resonance frequency, f_{LHR}, exceeds the frequencies of these waves,[16] as depicted schematically in Figure 6. (iv) The reflected waves propagate toward the equator in the narrow density-enhanced ducts whose upper cutoff is the half gyrofrequency of electron, $f_H/2$.[13,14,15]

Since $f_H' < f_H$, we can find, for example, the emissions produced with frequency $f \cong 0.55 f_H'$ (i.e., $f > f_H'/2$) arrive at the observing location with $f = 0.45 f_H$ (i.e., $f < f_H/2$), as indicated in Figure 6.

The present idea of the formation of the bimodal frequency distribution with a dip at $f_H/2$, which is also called "the band of missing emissions" in the geomagnetic equatorial whistler emissions such as chorus,[1,2,8] has other supporting evidence. These data which were observed by the OGO-3 satellite at the moment of the geomagnetic equatorial crossing on January 21, 1967[17] are shown in Figure 7. The magnetic latitudes corresponding to three figures are from the top approximately 0°, -2° and -5°, respectively, and an arrow in the left side of each figure indicates the frequency corresponding to $f_H/2$. From these figures, we can see the foliowing: (1) The emissions of $f > f_H/2$ are stronger and

more continuous than those of $f < f_H/2$, indicating emissions of $f > f_H/2$ are observed rather close to their sources. (2) The emissions of $f < f_H/2$ are striated, indicating these emissions are propagating in narrow ducts of enhanced ionization. (3) Most emissions are incoherent between the upper and lower frequencies, except the bottom example, which is rather non-equatorial, indicating that the sources of those two emissions are different or at least separated.

Further detail of the present theory which includes the growth rate of the emission based on the observed enhanced intensity and anisotropy of the low energy electrons, and the ray tracing of nonducting emissions produced with frequencies $f > f_H/2$ near the equator is being studied. Finally, it should be noticed that there are still additional effects on the formation of the missing emission band due to the interference of two modes of propagation for a frequency around $f \lesssim f_H/2$, as discussed by Burtis (1974)[17] and due to the Landau damping which dominates near the magnetic equator.[8,11] Investigations on the relation between the whistler mode emissions and the electrostatic mode emissions might bring another clue on these problems.

REFERENCES

1. Maeda, Kaichi, Planet. Space Sci., 24, 341 (1976)
2. Anderson, R. R. and Kaichi Maeda, to be published in J. Geophys. Res. (1976)
3. Parady, B. and L. J. Cahill, Jr., J. Geophys. Res., 78, 4765 (1973)
4. Anderson, R.R. and D. A. Gurnett, J. Geophys. Res., 78, 4756 (1973)
5. Kennel, C. F., F. L. Scarf, R. W. Fredricks, J. H. McGehee, and F. V. Coroniti, J. Geophys. Res., 75, 6136 (1970)
6. Bernstein, I. B., Phys. Rev., 109, 10 (1958)
7. Stix, T. H., Theory of Plasma Waves, McGraw Hill, N.Y. (1962)
8. Tsurutani, B. T. and E. T. Smith, J. Geophys. Res., 79, 118 (1974)
9. Gendrin, R., Space Sci. Rev., 18, 145 (1975)
10. Lyons, L. R. and D. J. Williams, J. Geophys. Res., 80, 943 (1975)
11. Liemohn, H. B., J. Geophys. Res., 72, 39 (1967)
12. Matsumoto, H. and I. Kimura, Planet. Space Sci., 19, 567 (1971)
13. Smith, R. L., R. A. Helliwell, and I. Yabroff, J. Geophys. Res., 65, 815 (1960)
14. Angerami, J. J., J. Geophys. Res., 75, 6115 (1970)
15. Helliwell, R. R., Whistlers and Related Ionospheric Phenomenon, Stanford Univ. Press (1965)
16. Kimura, I., Radioscience, 1, 269 (1966)
17. Burtis, J. W., Technical Report No. 3469-3, Stanford Radioscience Laboratories (1974)

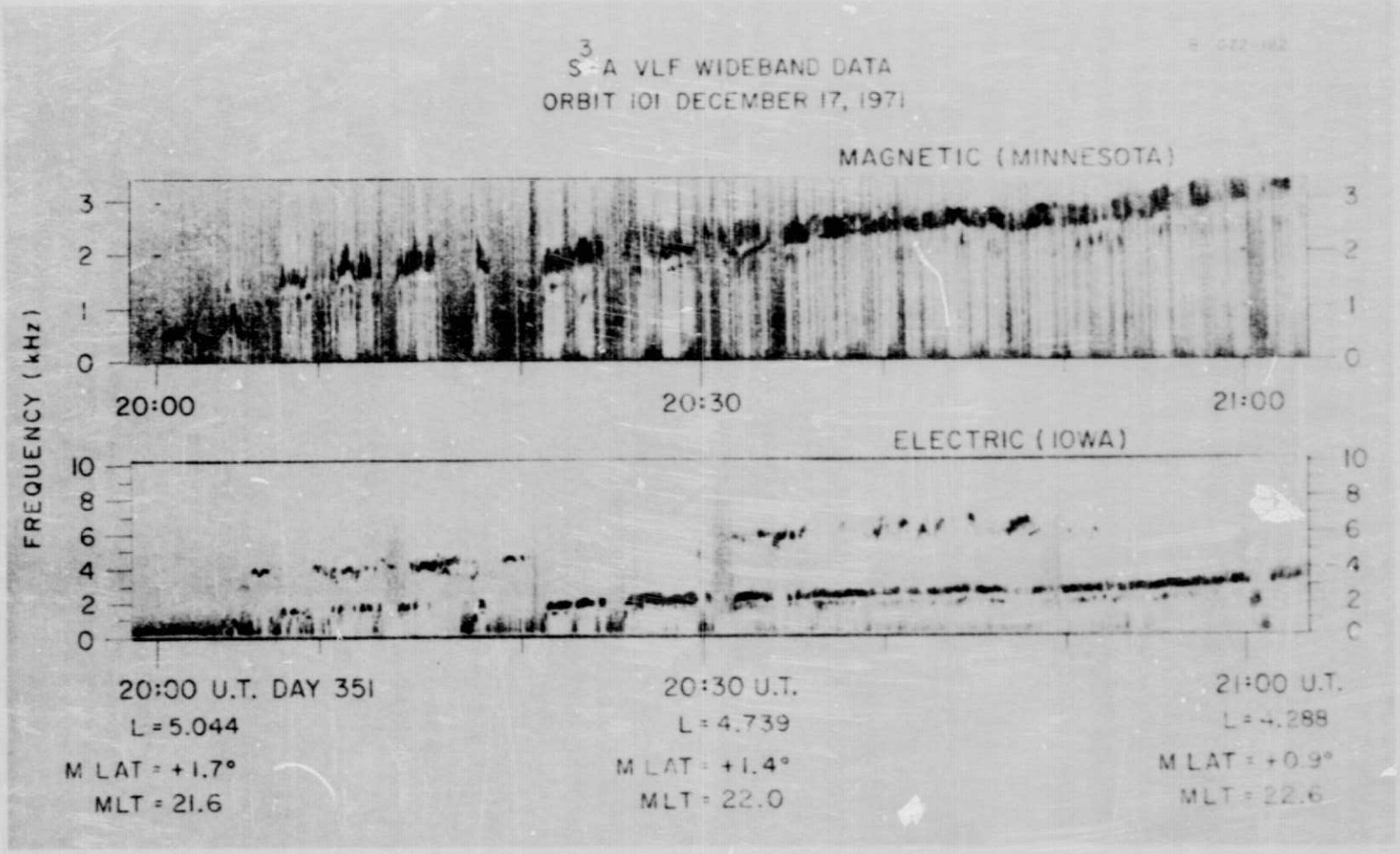

Figure 1. A part of the VLF-emission event observed by the S^3-A satellite (Explorer 45) during the main phase of the geomagnetic storm on December 17, 1971. The upper and lower figures indicate the emissions of the AC-magnetic field ($f \leq 3$ kHz) and the AC-electric field ($f \leq 10$ kHz), respectively. The numbers shown at the bottom are: (1) The universal time, U.T. (2) A measure of geocentric distance of the satellite in the equatorial plane, L (R_E units). (3) The magnetic latitude, M LAT. (4) The magnetic local time, MLT. The electron gyrofrequency, f_H, changes from 3.067 kHz at 20:00 UT to 3.662 kHz at 20:30 UT and to 5.386 kHz at 21:00 UT. Notice that there is a sharp gap along $f_H/2$ in the whistler mode emission and that the emissions above $f_H/2$ are stronger and more continuous than those below $f_H/2$.

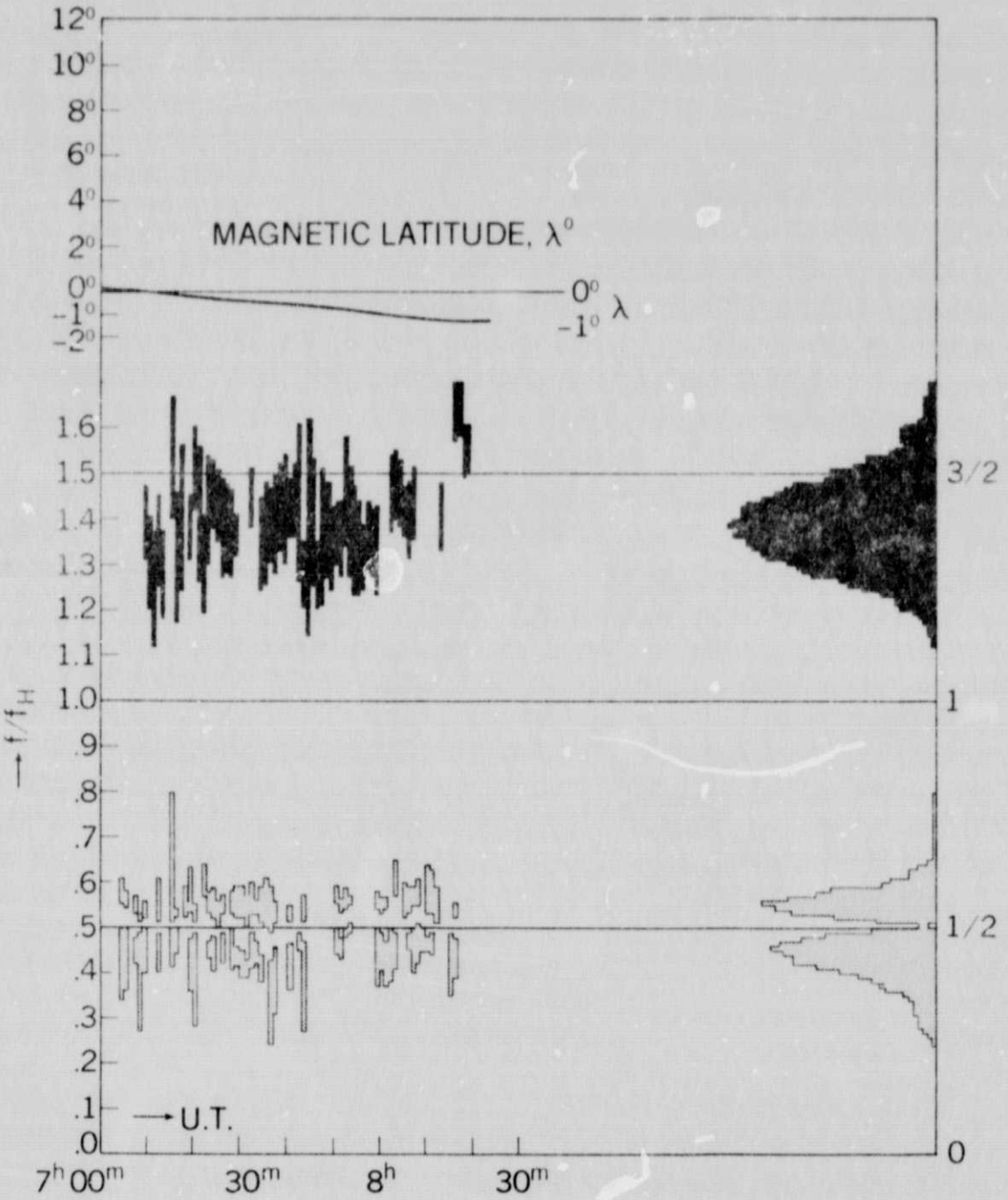

Figure 2. The frequency distribution of the VLF-emissions observed by the S3-A satellite during the substorm on January 22, 1972. The emission data are digitized by taking one-minute average values and normalized by f_H computed from the onboard magnetometer data. A line in the upper left indicates the latitude of the satellite during the emission event sh wn below. The frequency distributions made by accumulating the number of occurrence in each frequency interval ($\Delta f/f_H = 0.01$ is used) are shown on the right side of the figure. The bimodal frequency distribution with a conspicuous dip at exactly $f_H/2$ of the whistler mode emissions can be clearly noticed.

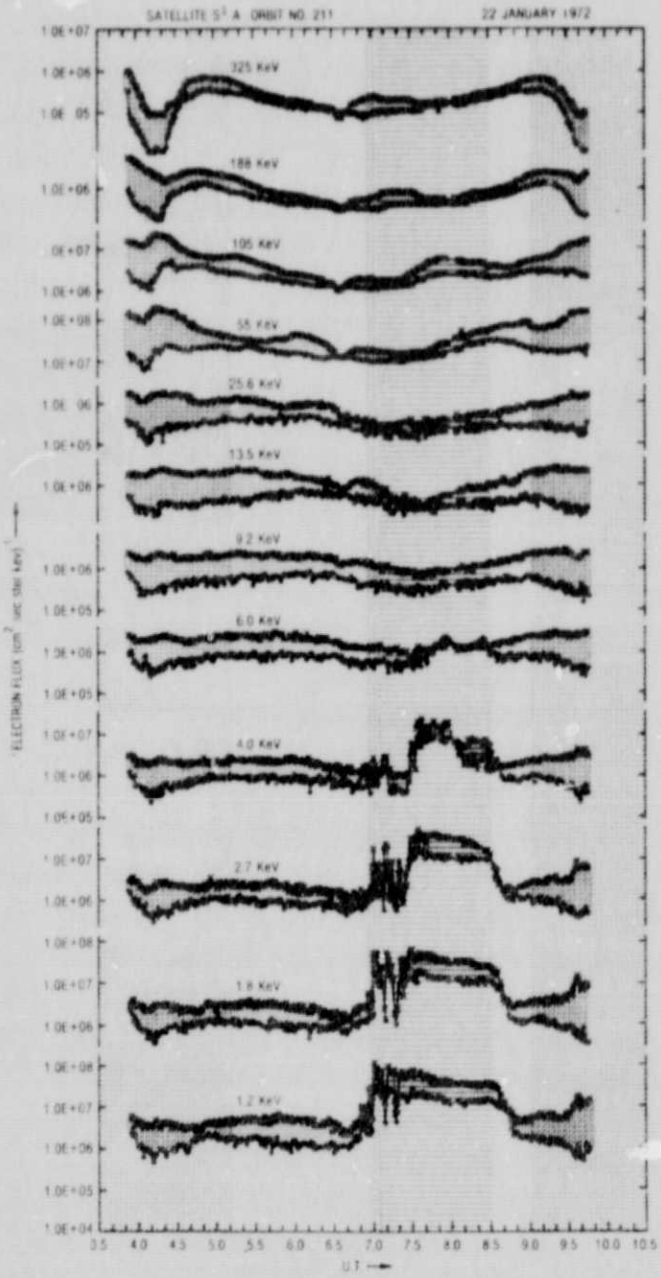

Figure 3. Variations of the directional differential electron intensities ($cm^{-2}sec^{-1}ster^{-1}keV^{-1}$) observed by the S^3-A satellite at the time of VLF-emission event occurred on January 22, 1972. Two lines for each energy, one with small crosses and the other with small circles, correspond to the intensities of 90° pitch angle and of the smallest observed pitch angle (closed to 25°), respectively. A time interval indicated by horizontal hatched lines corresponds to the period when the VLF-emissions shown in Figure 2 are observed. Other shaded time intervals correspond to the periods when the satellite is inside the plasmasphere.

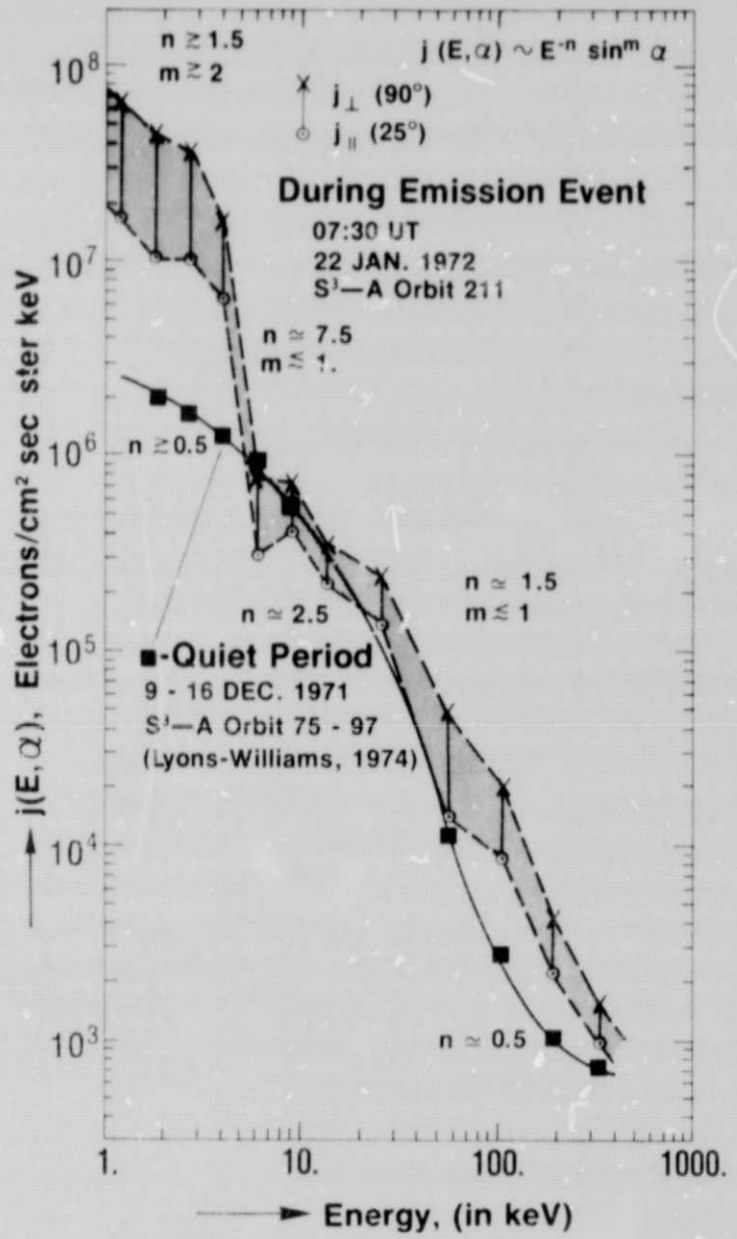

Figure 4. Differential energy spectra of the enhanced ring current electrons during the VLF-emission event (07:30 UT, 22 January 1972) in comparison with the mean quiet time spectrum given by Lyons and Williams.[10] Notice that the shaded part between two directional intensities manifests the anisotropy of the enhanced electron intensities at different energies. Approximating the energy spectrum and pitch angle dependence by $j(E,\alpha) \sim E^{-n}\sin^m\alpha$, the parameters n and m for three energy regimes are also indicated in the respective parts of the curves.

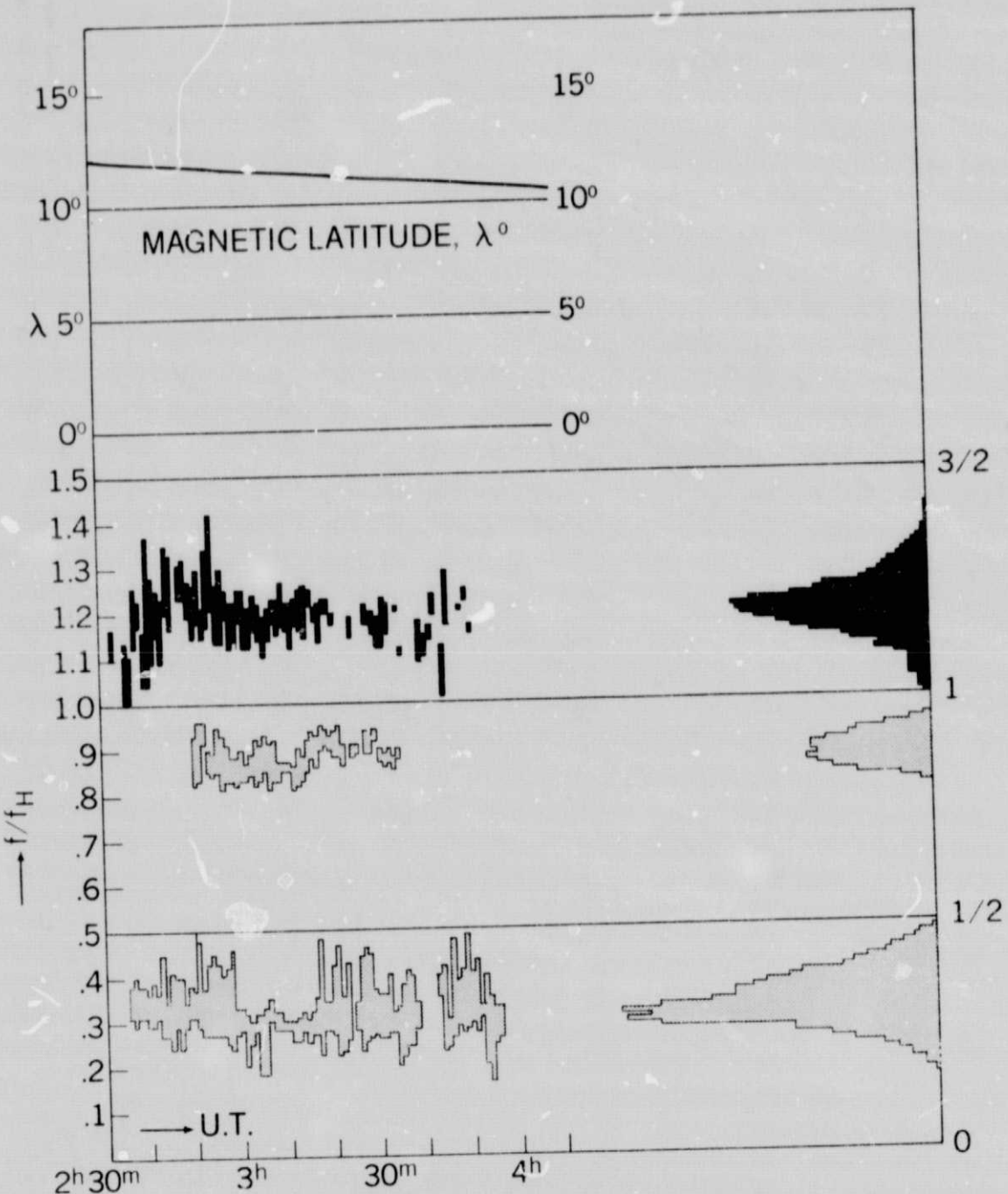

Figure 5. The normalized frequency distribution of the VLF-emission event observed off the equator by the S3-A satellite during the substorm on January 18, 1972. Notations are the same as used in Figure 2. Note that in this off-equatorial emission event, the emissions above $f_H/2$ are weaker than the emissions below $f_H/2$ and the frequencies are quite different from the near equatorial results shown in Figures 1 and 2.

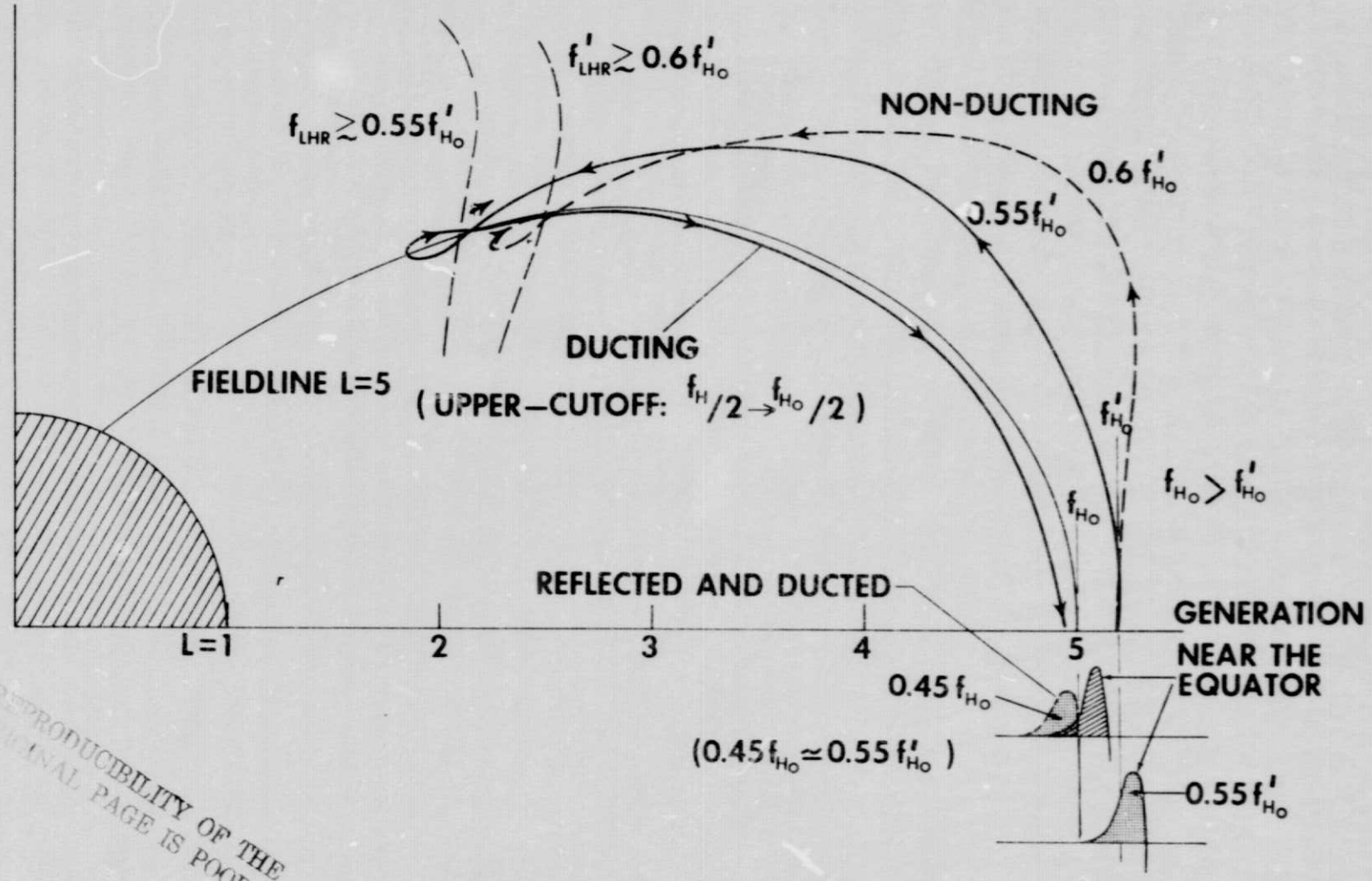

Figure 6. A schematic depiction of the formation of the bimodal frequency distribution in the magnetospheric VLF-emissions observed near the equator. (It should be noted that all ray paths are outside of the plasmasphere and that the loops of the propagation path at reflection points are exaggerated.)

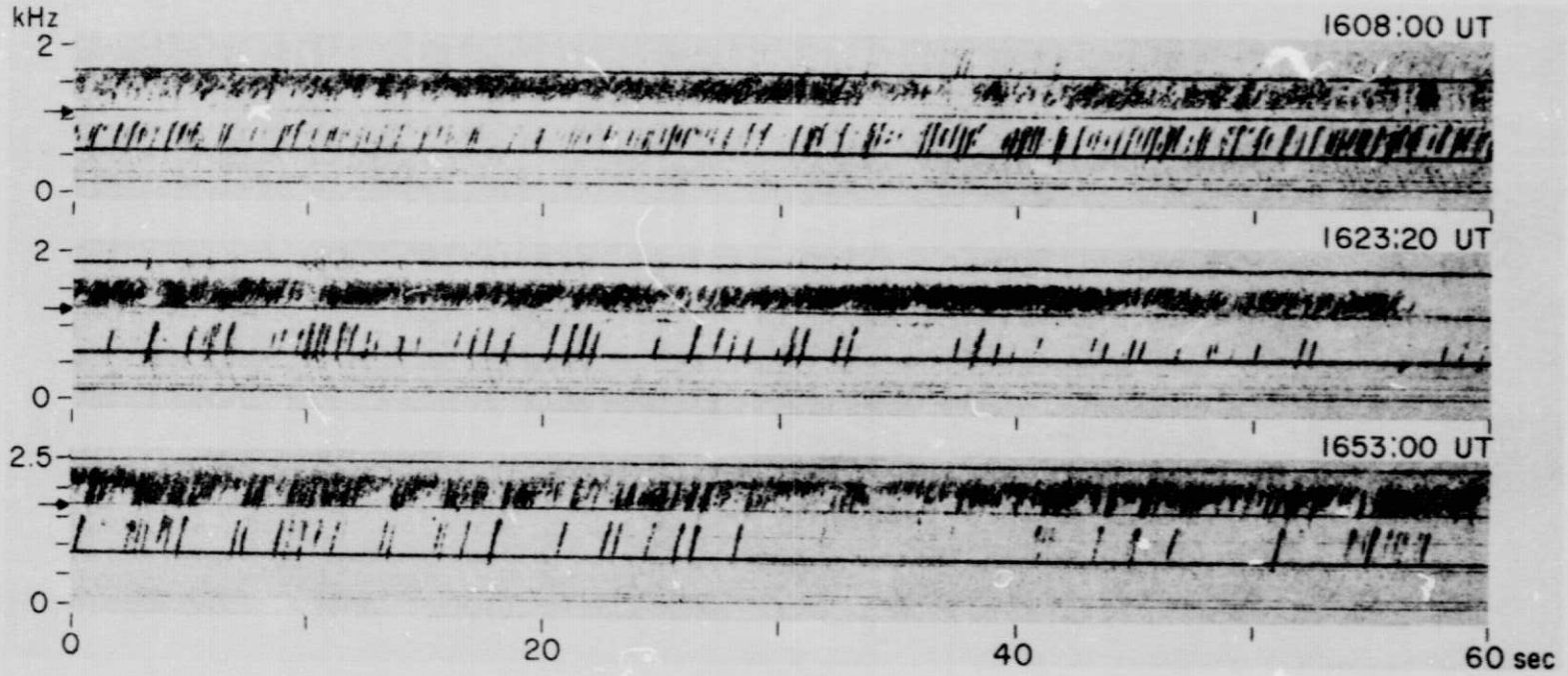

Figure 7. A portion of the VLF-emission data obtained by the OGO-3 satellite along its inbound crossing of the magnetic equator on January 21, 1967. The magnetic latitude of the three records is from top 0°, -2° and -5°, respectively. The arrows on the left side of the figure indicate the frequency of $f_H/2$. This figure is reproduced from the report written by Burtis[17] with the courtesy of Prof. R. R. Helliwell.